Development 139, 3553-3560 (2012) doi:10.1242/dev.077263

Celf1 regulation of *dmrt2a* is required for somite symmetry and left-right patterning during zebrafish development

Takaaki Matsui[1,*], Akihiro Sasaki[1], Naoko Akazawa[1], Hifumi Otani[2] and Yasumasa Bessho[1]

SUMMARY

RNA-binding proteins (RBPs) bind to numerous and diverse mRNAs to control gene expression post-transcriptionally, although the in vivo functions of specific RBP-mRNA interactions remain largely unknown. Here, we show that an RBP named Cugbp, Elav-like family member 1 (Celf1) controls expression of a gene named *doublesex and mab-3 related transcription factor 2a* (*dmrt2a*), which is essential for somite symmetry and left-right patterning during zebrafish development. Celf1 promotes *dmrt2a* mRNA decay by binding to UGU repeats in the 3′UTR of *dmrt2a* mRNA such that *celf1* overexpression reduces the amount of *dmrt2a* mRNA, leading to asymmetric somitogenesis and laterality defects. Furthermore, blocking the Celf1-*dmrt2a* mRNA interaction by a target protector morpholino alleviates failures in somite symmetry and left-right patterning that are caused by *celf1* overexpression. Our results therefore demonstrate that Celf1-dependent fine-tuning of *dmrt2a* expression is essential for generating bilateral symmetry of somites and left-right asymmetric patterning during zebrafish development.

KEY WORDS: RNA-binding protein, Post-transcriptional regulation, Symmetric somitogenesis, Left-right patterning, Target protector morpholino, Zebrafish

INTRODUCTION

Transcriptional control has important roles in generating a properly organized body during vertebrate development (Naiche et al., 2005; Schier and Talbot, 2005; Shivdasani, 2002). However, levels of particular transcripts are highly variable in space and time during development because of the stochastic nature and the spatiotemporal regulation of transcription (Blake et al., 2003; Elowitz et al., 2002). Embryos must therefore have systems that precisely control the amounts of proteins, to regulate multiple developmental processes at post-transcriptional levels (Gebauer and Hentze, 2004). RNA-binding proteins (RBPs) are known to provide such a mechanism. For instance, an RBP named Cugbp Elav-like family member 1 (Celf1) controls gene expression at multiple post-transcriptional levels, including alternative splicing, deadenylation and mRNA decay, and fine-tunes the abundance of proteins that are synthesized from its target mRNAs (Barreau et al., 2006; Vlasova et al., 2008).

Celf1 target mRNAs have been identified by a yeast three-hybrid screen, a SELEX (systematic evolution of ligands by exponential enrichment) approach, an in vitro binding assay and RNA immunoprecipitation assays (Lee et al., 2010; Marquis et al., 2006; Mori et al., 2008; Rattenbacher et al., 2010; Suzuki et al., 2002; Takahashi et al., 2000). In HeLa cells, Celf1 binds to >600 short-lived mRNAs that are involved in cell growth, motility and apoptosis (Rattenbacher et al., 2010), suggesting that Celf1 coordinately regulates protein expression from multiple mRNAs. Analyses of the conserved sequences among these mRNAs reveal that UG-rich elements or UGU repeats, such as UGUUUGUUUGU and UGUGUGUGUGU, are the binding sequences of Celf1 (Rattenbacher et al., 2010); these sequences are similar to target elements identified by other methods in human, mouse and frog (Lee et al., 2010; Marquis et al., 2006; Mori et al., 2008; Takahashi et al., 2000).

Celf1 is broadly expressed in early vertebrate embryos, whereas *Celf1* expression is restricted to specific regions, such as eyes and somites (Gautier-Courteille et al., 2004; Hashimoto et al., 2006; Kress et al., 2007), suggesting a role(s) for Celf1 in the regulation of developmental processes. However, loss of *Celf1* function in either frog or mouse embryos has only minor effects on their development; knockdown of the *Xenopus Celf1* ortholog *EDEN-BP* results in only a defect of somite segmentation (Gautier-Courteille et al., 2004). Some *Celf1*-knockout mice are viable to the adult stage, although they display growth retardation (Kress et al., 2007). These mild effects on development may be explained by redundant actions among Celfs and/or by high abundance of proteins synthesized from Celf1 target mRNAs. Therefore, the physiological roles for *Celf1* in the regulation of vertebrate development remain largely unclear.

A possible strategy to explore such a role for *Celf1* is to deplete proteins synthesized from Celf1 target mRNAs. We thus overexpressed *celf1* in zebrafish embryos to intensify Celf1-mediated post-transcriptional regulation. This manipulation resulted in failures of bilateral symmetric somitogenesis and left-right (LR) asymmetric patterning, defects which are similar to the phenotype induced by knockdown of a single gene named *doublesex and mab-3 related transcription factor 2a* (*dmrt2a*, formerly *terra*) (Saude et al., 2005). We also found that Celf1 downregulates *dmrt2a* expression by binding to the 3′UTR of *dmrt2a* mRNA. Furthermore, blocking the interaction between Celf1 and *dmrt2a* mRNA reduced the effects of *celf1* overexpression on both somite symmetry and LR asymmetric patterning. Our results therefore identify a crucial role of the specific Celf1-mRNA pair in generating a properly organized body during vertebrate development, and provide a powerful tool for analyzing the roles of specific RBP-mRNA pairs in various experimental settings.

[1]Gene Regulation Research, Graduate School of Biological Sciences, Nara Institute of Science and Technology, 8916-5 Takayama, Nara 630-0101, Japan. [2]Cooperative Research Division, Nara Institute of Science and Technology, 8916-5 Takayama, Nara 630-0101, Japan.

*Author for correspondence (matsui@bs.naist.jp)

Accepted 1 July 2012

MATERIALS AND METHODS

Zebrafish and whole-mount in situ hybridization

Wild-type zebrafish were used in this study. Whole-mount in situ hybridization was performed as described previously (Matsui et al., 2005; Matsui et al., 2011). cDNA fragments of *celf1*, *dlx3*, *dmrt2a*, *her1*, *hgg1* (*ctsl1b* – Zebrafish Information Network), *mlc2a* (*mgl7* – Zebrafish Information Nework), *myod*, *ntl*, *pitx2a* and *uncx4.1* were used as templates for the antisense probes.

mRNA and morpholino injections

pCS2-*celf1* (long form), pCS2-*celf1*$^{\Delta linker}$, pCS2-*dmrt2a* and pCS2-*monomeric red fluorescent protein* (*mRFP*) were used in this study. *celf1*, *celf1*$^{\Delta linker}$, *dmrt2a* and *mRFP* mRNA were synthesized using the SP6 mMessage mMachine System (Ambion). Either 50 or 150 pg *celf1* mRNA was injected into one-cell-stage zebrafish embryos; as a control, either 50 or 150 pg *mRFP* mRNA was injected.

Because a deletion mutant of the linker domain of human or frog Celf1 (Celf1$^{\Delta linker}$) is known to lose its functional activity by losing RNA-binding activity or by preventing oligomerization (Takahashi et al., 2000; Cosson et al., 2006), we used zebrafish *celf1*$^{\Delta linker}$ as a negative control in this study. To confirm its protein expression in embryos, we injected 50 pg *celf1*$^{\Delta linker}$ mRNA into one-cell-stage zebrafish embryos, and found that a 26 kDa protein, equivalent to that of mutant protein, was expressed in the manipulated embryos (supplementary material Fig. S1B). To test its functional activity, we performed quantitative PCR for *dmrt2a* in *celf1*$^{\Delta linker}$-overexpressing embryos and showed that Celf1$^{\Delta linker}$ does not affect *dmrt2a* expression in vivo (Fig. 5A). These observations suggest that Celf1$^{\Delta linker}$ acts as a loss-of-function mutant in our experimental settings.

To generate a Celf1-resistant *dmrt2a* mRNA, we engineered the plasmid pCS2-*dmrt2a*, which harbors only the coding region of *dmrt2a* and does not include the Celf1-binding site within the 3′UTR. We thus used mRNA synthesized from the pCS2-*dmrt2a* as the Celf1-resistant *dmrt2a* mRNA.

Antisense MO oligonucleotides named *celf1_long*-MO, *celf1_short*-MO, *dmrt2a*-MO, *dmrt2a*-TP-MO or control-MO were obtained from Gene Tools. *celf1_long*-MO, *celf1_short*-MO and *dmrt2a*-MO were designed to target the AUG initiation codon of these mRNAs. *dmrt2a*-TP-MO was designed to target the UGU repeats within the 3′UTR of *dmrt2a* mRNA.

The MO sequences were as follows: control-MO, 5′-CCTC-TTACCTCAGTTACAATTTATA-3′; *celf1_long*-MO, 5′-GCTTCAGC-TTCGATACTATCCATCC-3′; *celf1_short*-MO, 5′-GTGGTCCAGAGA-CCCATTCATCTTC-3′; *dmrt2a*-MO, 5′-AGATCCGTCATTTTCTGGCC-GCGTA-3′ (Saude et al., 2005); *dmrt2a*-TP-MO, 5′-ACATTTAC-AATTAAATACTCTACAC-3′.

To knock down *celf1*, we co-injected 2.5 ng *celf1_long*-MO and 2.5 ng *celf1_short*-MO (5 ng *celf1*-MOs) into one-cell-stage zebrafish embryos. To protect *dmrt2a* mRNA from Celf1, we injected 5 ng *dmrt2a*-TP-MO into one-cell-stage zebrafish embryos; as a control, we injected 5 ng control-MO. To confirm the specificity of *dmrt2a*-TP-MO, *dmrt2a*-TP-MO (5 ng) was co-injected with either *dmrt2a*-MO (0.5 ng and 1 ng) or control-MO (1 ng) into one-cell-stage embryos. For rescue experiments, a combination of *celf1* mRNA (50 pg) with either *dmrt2a*-TP-MO (2.5 ng and 5 ng), control-MO (5 ng), *dmrt2a* mRNA (1.25 pg and 2.5 pg) or *mRFP* mRNA (2.5 pg) were co-injected into one-cell-stage embryos. Defects of somite symmetry and LR patterning in these embryos were evaluated by in situ hybridization for *uncx4.1* and *mlc2a*, respectively.

The specificity and efficacy of *celf1_long*-MO and *celf1_short*-MO was tested by co-injection of RNAs encoding GFP-tagged celf1_long or celf1_short (*celf1L-GFP* or *celf1S-GFP*) with the cognate MO into zebrafish embryos and by western blotting using anti-Celf1 antibody, respectively (supplementary material Fig. S1B). The efficacy of *dmrt2a*-MO was confirmed in vivo by its ability to recapitulate the phenotype of *dmrt2a* morphants, as shown previously (Saude et al., 2005). The efficacy and specificity of *dmrt2a*-TP-MO were evaluated by RNA immunoprecipitation assay and quantitative PCR assay (Fig. 4C, Fig. 5A).

Western blotting

Embryos at 12-14 hours post-fertilization (hpf) were squeezed using glass slides to remove the yolk and to dissociate cells. Dissociated cells were lysed with lysis buffer (PBS containing 1% Triton X-100, 0.2% SDS, 150 mM NaCl and 5 mM EDTA). Cell lysates were subjected to SDS-PAGE, and then transferred to Hybond-P membrane (GE Healthcare). To detect Celf1, the membrane was incubated with rabbit anti-Celf1 antiserum (a gift from Dr Kunio Inoue, Kobe University, Japan). After extensive washing, the membrane was incubated with HRP-conjugated anti-rabbit antibody (Jackson ImmunoResearch Laboratories), and the immune complex was visualized with ChemiLumi One L (Nacalai Tesque). After stripping, the membrane was incubated with mouse anti-β-actin antibody (Sigma), and then with HRP-conjugated anti-mouse antibody (Jackson ImmunoResearch Laboratories).

In vitro binding assay

Cos7 cells were transfected with pCS2-*celf1* using Trans-IT LT-1 (Mirus) according to the manufacturer's protocol. After 48 hours cultivation, cells were lysed with binding buffer [10 mM Tris-HCl (pH8.0), 150 mM NaCl, 1 mM $MgCl_2$, 0.1 mM $CaCl_2$, 0.5% NP-40 and 5% glycerol]. Biotinylated RNA oligonucleotides (Gene Design) were pre-mixed with streptavidin-Sepharose beads (GE Healthcare) for 10 minutes, and mixed with cell lysate for 30 minutes at room temperature. The beads were washed three times with binding buffer, and pulled-down proteins were subjected to western blotting using anti-Celf1 antiserum.

The sequences of RNA oligonucleotides were as follows: *dmrt2a*_wildtype, 5′-auguguagaguauuuaauuguaaauguuaauuuug-3′; *dmrt2a*_3p mut, 5′-augCguagaguauuuaauCgCaaauguuaauuuug-3′; *dmrt2a*_7p mut, 5′-aCgCgCagaguauuuaauCgCaaaCgCuaauuuug-3′; s0 (negative control), 5′-aguacucgacgggacggcugcugugaacgacuacg-3′ (Marquis et al., 2006); EDEN (positive control), 5′-guauauguauguguuguuuuauuguguguguguu-3′ (Marquis et al., 2006) (intact nucleotides in lower case, substituted nucleotides in uppercase).

RNA immunoprecipitation (RIP)

According to the manufacturer's protocol of the RIP-Assay Kit (MBL), complexes that consist of mRNAs and Celf1 were isolated from either uninjected embryos or *dmrt2a*-TP-MO-injected embryos at 12-14 hpf using rabbit anti-Celf1 antiserum. Normal rabbit serum (Thermo Scientific) was used as a control. In vivo interaction between Celf1 and *dmrt2a* mRNA, *myod* mRNA, a known target of Celf1 in a mouse myoblast cell line named C2C12 (Lee et al., 2010), or *suppressor of hairless* (*rbpja* or *rbpjb* in zebrafish) mRNA, a known target in frog (Cibois et al., 2010; Gautier-Courteille et al., 2004), was tested by quantitative PCR (see below). We also tested interaction of Celf1 with non-target mRNAs (*β-actin* and *cyclinA1*) as negative controls.

Quantitative PCR (qPCR) and measurement of mRNA half life

Embryos injected with control-MO, *celf1*-MOs or *dmrt2a*-TP-MO were grown to 12-14 hpf. To measure mRNA half life, embryos injected with control-MO, *celf1*-MOs or *dmrt2a*-TP-MO were grown to 11 hpf, treated with 8 μg/ml Actinomycin-D (Nacalai Tesque) for 1 hour and collected at the indicated time points following the incubation.

Total RNAs of embryos were isolated using Sepasol RNA I (Nacalai Tesque). First-strand cDNAs were synthesized from total RNA with SuperScript II (Invitrogen) and oligo-dT primers (Invitrogen). Quantitative real-time PCR using gene-specific primers (see below) was performed in either MX3000p (Agilent Technologies) using SYBR-Green PCR Master Mix (Takara Bio) or LightCycler 480 system II (Roche Diagnostics) using LightCyclar 480 SYBR Green I Master (Roche Diagnostics).

The sequences of gene-specific primers were as follows: *dmrt2a*-F, 5′-CGTTTGTTTGACTGCTTTGG-3′; *dmrt2a*-R, 5′-CGCCTGATC-ATCGCTCTC-3′; *myod*-F, 5′-ACTTCAATGACACACCAAATG-3′; *myod*-R, 5′-CATGCAGGAGTCTCTGTGGA-3′; *rbpja*-F, 5′-TTTACGC-CCAACCTCAGAGT-3′; *rbpja*-R, 5′-ACGCAGAGATGTCAGGAACC-3′; *rbpjb*-F, 5′-ACAGAACTTCTCTCCAACTCTGC-3′; *rbpjb*-R, 5′-ATGCTCTCCCCACACCTG-3′; *cyclin A1*-F, 5′-CAATATCTGC-CATCCAAGACC-3′; *cyclin A1*-R, 5′-AATCACAGCCAG-AGAGTAACCAG-3′; *β-actin*-F, 5′-GCTGTTTTCCCCTCCATTGTTG-3′; *β-actin*-R, 5′-TTTCTGTCCCATGCCAACCAT-3′.

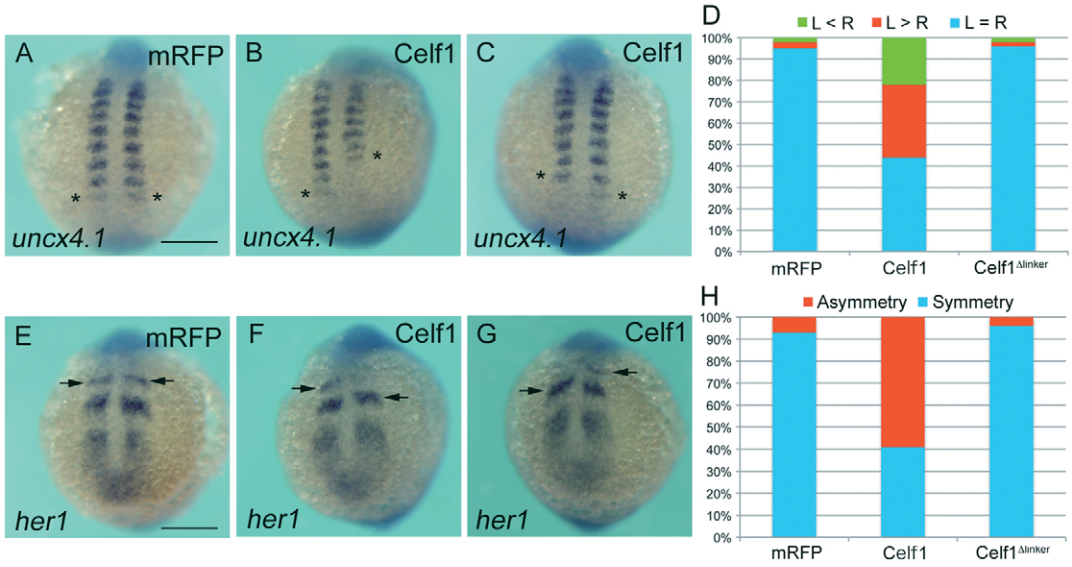

Fig. 1. Overexpression of *celf1* leads to defects in bilateral symmetry of the somites. (**A-C**) Representative images of *uncx4.1* expression demonstrating symmetric (mRFP; A), left-biased (Celf1; B) or right-biased (Celf1; C) asymmetric somitogenesis in zebrafish embryos at 12-14 hpf. Dorsal view, anterior to the top. Asterisks mark the last-formed somite. (**D**) Percentages of symmetric (L=R), left-biased (L>R) or right-biased (L<R) asymmetric somitogenesis in *mRFP*- (n=60), *celf1*- (*n*=89) or *celf1*$^{\Delta linker}$- (*n*=60) overexpressing embryos. (**E-G**) Representative images of *her1* expression demonstrating symmetric (mRFP; E) or asymmetric (Celf1; F,G) oscillation in embryos at 12-14 hpf. Arrows indicate the position of the anterior strip of *her1*. Vegetal pole view. (**H**) Percentages of symmetric and asymmetric *her1* oscillation in *mRFP*- (*n*=87), *celf1*- (*n*=98) or *celf1*$^{\Delta linker}$- (*n*=76) overexpressing embryos. Scale bars: 200 μm.

RESULTS

celf1 controls somite symmetry and LR asymmetric patterning in zebrafish

Overexpression of *celf1*, by injection of 50 pg *celf1* mRNA into one-cell-stage zebrafish embryos, often resulted in an uneven number of somites on the left and right sides at 12-14 hpf (56%, *n*=89; Fig. 1B-D). Sixty percent of the defective embryos had one or more excess somites on the left side (Fig. 1B,D) and 40% had an excess on the right side (Fig. 1C,D), suggesting that this asymmetry was not biased towards either side. However, injection of 50 pg *celf1*$^{\Delta linker}$ mRNA, which encodes a loss-of-function mutant of Celf1 (for details, see Materials and methods), did not alter somite symmetry (Fig. 1D). As LR asymmetric somitogenesis can be caused by loss of synchrony of the segmentation clock, including the Notch effector *her1*, between the left and right presomitic mesoderm (Kawakami et al., 2005; Saude et al., 2005;

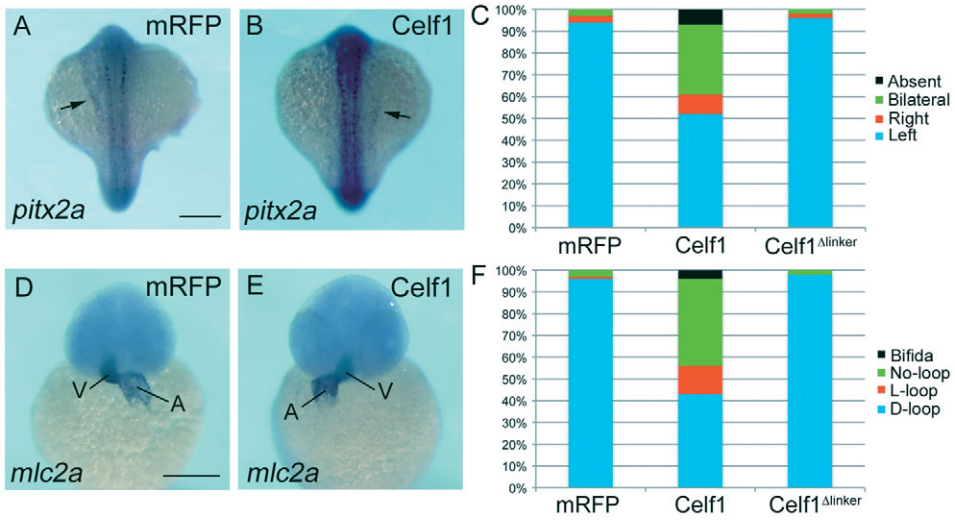

Fig. 2. Overexpression of *celf1* results in failures of LR asymmetric patterning. (**A**,**B**) Representative images showing left- (mRFP; A) or right- (Celf1; B) sided expression of *pitx2a* in zebrafish embryos at 18-19 hpf. Dorsal view, anterior to the top. Arrows indicate *pitx2a* expression in the lateral plate mesoderm. (**C**) Percentages of left-sided, right-sided, bilateral, or no (absent) expression of *pitx2a* in *mRFP*- (*n*=92), *celf1*- (*n*=102) or *celf1*$^{\Delta linker}$- (*n*=55) overexpressing embryos. (**D**,**E**) Representative images of m*lc2a* expression showing D-loop (mRFP; D) or L-loop (Celf1; E) of the heart in embryos at 42-45 hpf. Ventral view, anterior to the top. A, atrium; V, ventricle. (**F**) Percentages of D-loop, L-loop, no-loop or cardia bifida of the heart in *mRFP*- (*n*=92), *celf1*- (*n*=102) or *celf1*$^{\Delta linker}$- (*n*=51) overexpressing embryos. Scale bars: 200 μm.

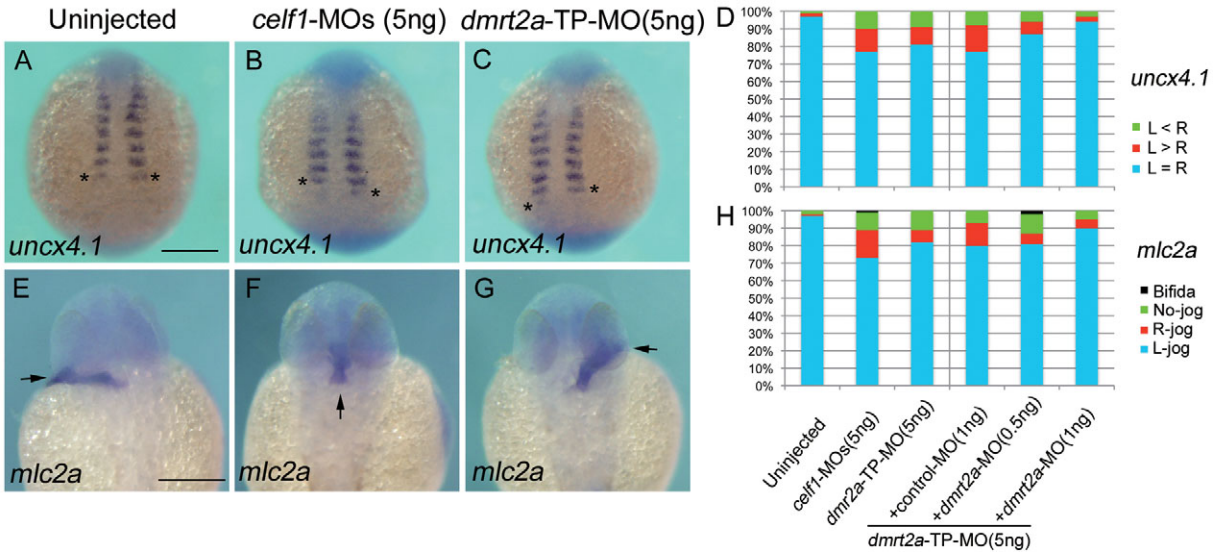

Fig. 3. Knockdown of *celf1* leads to defects in somite symmetry and LR patterning. (**A-C**) Representative images of *uncx4.1* expression demonstrating symmetric (uninjected; A), right-biased (*celf1*-MOs; B) or left-biased (*dmrt2a*-TP-MO; C) asymmetric somitogenesis in zebrafish embryos at 12-14 hpf. Dorsal view, anterior to the top. Asterisks mark the last-formed somite. (**D**) Percentages of symmetric (L=R), left-biased (L>R) or right-biased (L<R) asymmetric somitogenesis in embryos injected with 5 ng control-MO (*n*=121), 5 ng *celf1*-MOs (*n*=102), 5 ng *dmrt2a*-TP-MO (*n*=90), 5 ng *dmrt2a*-TP-MO plus 1 ng control-MO (*n*=40), 5 ng *dmrt2a*-TP-MO plus 0.5 ng *dmrt2a*-MO (*n*=60) or 5 ng *dmrt2a*-TP-MO plus 1 ng *dmrt2a*-MO (*n*=68). (**E-G**) Representative images of m*lc2a* expression showing L-jog (uninjected; E), no-jog (*celf1*-MOs; F) or R-jog (*dmrt2a*-TP-MO; G) of the heart in embryos at 24-28 hpf. Dorsal view, anterior to the top. Arrows indicate the direction of heart jogging. (**H**) Percentages of L-jog, R-jog, no-jog or cardia bifida of the heart in embryos injected with 5 ng control-MO (*n*=152), 5 ng *celf1*-MOs (*n*=90), 5 ng *dmrt2a*-TP-MO (*n*=76), 5 ng *dmrt2a*-TP-MO plus 1 ng control-MO (*n*=46), 5 ng *dmrt2a*-TP-MO plus 0.5 ng *dmrt2a*-MO (*n*=47) or 5 ng *dmrt2a*-TP-MO plus 1 ng *dmrt2a*-MO (*n*=46). Scale bars: 200 μm.

Vermot et al., 2005; Vermot and Pourquie, 2005), we investigated next whether *celf1* overexpression affects the synchrony of *her1* oscillatory expression. *her1* oscillation was observed in all *celf1*-overexpressing embryos, but more than half of the embryos showed asynchronous *her1* oscillation between the left and right presomitic mesoderm (58%, *n*=98; Fig. 1F-H).

Defects in LR axis determination yield an uneven number of somites without bias to either side (Kawakami et al., 2005; Oishi et al., 2006; Saude et al., 2005). By contrast, loss of retinoic acid signaling leads to strongly biased asymmetric somitogenesis: almost all embryos have excess somites on the left side (Kawakami et al., 2005; Vermot et al., 2005; Vermot and Pourquie, 2005;

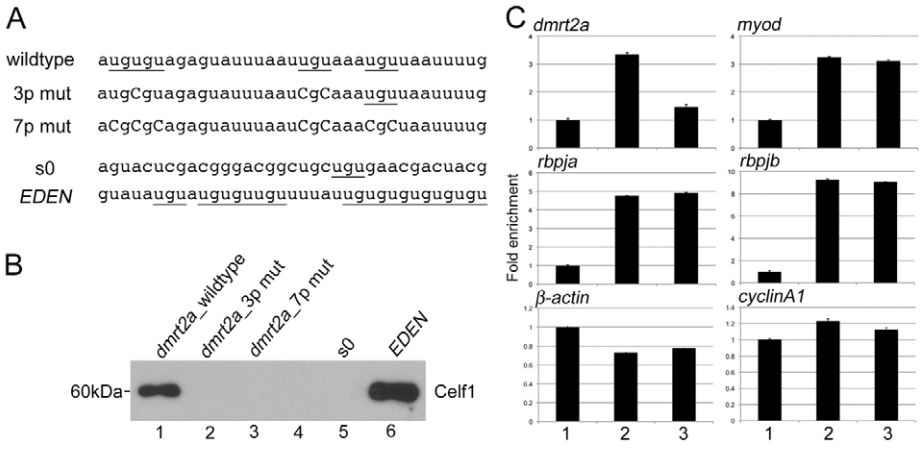

Fig. 4. Celf1 binds to *dmrt2a* mRNA in vitro and in vivo. (**A**) Sequences of RNA oligonucleotide probes used in vitro binding assay. Underlines mark UGU repeats and capital letters indicate substituted nucleotides. (**B**) Binding of Celf1 with specific RNA was tested by in vitro binding assay. Lane 1: *dmrt2a*_wildtype; lane2: *dmrt2a*_3p mut; lane 3: *dmrt2a*_7p mut; lane 4: empty; lane 5: s0 (negative control); lane 6: *EDEN* (positive control). Interaction between Celf1 and either *dmrt2a*_wildtype (lane 1) or *EDEN* (lane 6) was detected. (**C**) In vivo interaction between Celf1 with *dmrt2a* (upper left panel), *myod* (upper right panel), *rbpja* (middle left panel), *rbpja* (middle right panel), *β-actin* (lower left panel) or *cyclinA1* (lower right panel) mRNAs. Column 1: RIP control sample using normal serum from uninjected embryos; column 2: RIP sample using Celf1 antiserum (Celf1 AS) from uninjected embryos; column 3: RIP sample using Celf1 AS from embryos injected with *dmrt2a*-TP-MO. Celf1 interacted with *dmrt2a*, *myod*, *rbpja* and *rbpjb* mRNAs. *dmrt2a*-TP-MO specifically blocked the interaction of Celf1 with *dmrt2a* mRNA.

Vilhais-Neto et al., 2010). Because *celf1* overexpression led to unbiased somite asymmetry (Fig. 1B-D), we reasoned that *celf1* overexpression resulted in a failure of LR axis determination, leading to asymmetric somitogenesis. To test this, we investigated laterality in either *celf1*- or *celf1*$^{\Delta linker}$-overexpressing embryos. Left-sided expression of *pitx2a* in the lateral plate mesoderm was randomized in *celf1*-overexpressing embryos but not in *celf1*$^{\Delta linker}$-overexpressing embryos (Fig. 2B,C). Consistent with this phenotype, cardiac laterality evaluated by expression of *myosin light chain 2a* (*mlc2a*) was also randomized only in *celf1*-overexpressing embryos (Fig. 2E,F). These results suggest that *celf1* overexpression fails to determine proper LR axis, eventually leading to unbiased somite asymmetry as well as laterality defects.

To investigate the endogenous role of *celf1*, we knocked down *celf1* in zebrafish embryos using antisense morpholino oligonucleotides (MOs). Because two forms of Celf1 (long and short) are expressed in zebrafish (Hashimoto et al., 2006), MOs for long and short forms of *celf1* (*celf1_long*-MO and *celf1_short*-MO) were used in this study (for details, see Materials and methods and supplementary material Fig. S1A,B). Almost all *celf1* morphants showed somite segmentation defects (94%, *n*=88; supplementary material Fig. S1C,D) similar to the phenotype induced by knockdown of *EDEN-BP* in frog (Gautier-Courteille et al., 2004). In addition, 22-28% of *celf1* morphants displayed defects in somite symmetry and LR asymmetric patterning (Fig. 3B,D,F,H). These results indicate that Celf1 is essential for generating proper somite symmetry and LR asymmetric body plan.

Celf1 binds to *dmrt2a* mRNA in vitro and in vivo

Celf1 acts as a negative regulator of gene expression by binding to specific mRNAs (Lee et al., 2010; Marquis et al., 2006; Mori et al., 2008; Rattenbacher et al., 2010; Suzuki et al., 2002; Takahashi et al., 2000). Based on our data and these findings, we anticipated that knockdown of target genes would yield similar defects to those seen in *celf1*-overexpressing embryos. To identify such a target(s), we undertook a search for genes involved in both somite symmetry and LR asymmetric patterning. We found putative Celf1-binding sites in several genes, including *wnt11*, *duboraya*, *one-eyed pinhead*, *no tail* and *dmrt2a*, that are involved in LR patterning. However, the knockdown phenotypes of *wnt11*, *duboraya*, *one-eyed pinhead* or *no tail* are different from those of *celf1* overexpression, suggesting that these genes are unlikely to be the target of Celf1 in the context of somite symmetry and LR patterning. As a candidate, we selected *dmrt2a* for the following three reasons: (1) knockdown of *dmrt2a* in zebrafish embryos results in laterality defects as well as an uneven number of somites without bias (Saude et al., 2005) (supplementary material Fig. S2); (2) expression of *dmrt2a* is detected in the somites, the presomitic mesoderm and the tailbud, where *celf1* is also expressed (Meng et al., 1999) (supplementary material Fig. S3A); and (3) a putative Celf1-binding site containing four UGU repeats and U- and A-rich sequences within 35 nucleotides is present in the 3′ UTR of *dmrt2a* mRNA (supplementary material Fig. S3C).

Because in situ hybridization confirmed that *celf1* and *dmrt2a* expression overlap in the tailbud and the somites at 12-14 hpf (supplementary material Fig. S3A,B), we performed further experiments to elucidate the relationship between Celf1 and *dmrt2a* mRNA. In vitro binding assays using biotinylated RNA probes revealed that Celf1 associated with the putative binding site in the 3′UTR of *dmrt2a* mRNA (Fig. 4B, lane 1), but not with mutated sequences in which all or three UGU repeats were disrupted (Fig. 4B, lanes 2 and 3), indicating that Celf1 binds to the UGU repeats in the 3′UTR of *dmrt2a* mRNA. To examine whether endogenous Celf1 also binds to *dmrt2a* mRNA in zebrafish embryos, we performed RNA immunoprecipitation (RIP) of Celf1-mRNA complexes in embryos at 12-14 hpf. RIP using Celf1 antiserum led to a 3.3-fold enrichment of *dmrt2a* mRNA relative to negative control using normal serum (Fig. 4C). The integrity of the RIP assay was ensured by testing whether Celf1 interacts with either its known targets including *myod* or *rbpj* (*rbpja* or *rbpjb*) (Cosson et al., 2006; Takahashi et al., 2000), which harbor the putative Celf1-binding sites within the 3′UTR (supplementary material Fig. S3D,E), or non-targets such as *β-actin* and *cyclin A1* (Fig. 4C).

Celf1 controls *dmrt2a* mRNA decay in vivo

To test whether the interaction between Celf1 and *dmrt2a* mRNA affects *dmrt2a* expression, we examined the amounts of *dmrt2a* mRNA in either *celf1* morphants or *celf1*-overexpressing embryos by qPCR. *celf1* knockdown resulted in a 57% increase of the amount of *dmrt2a* mRNA relative to embryos injected with control-MO (Fig. 5A). Conversely, *celf1* overexpression led to a 50% reduction of *dmrt2a* mRNA relative to control mRFP overexpression (Fig. 5A). In addition, qPCR analyses in *celf1* morphants treated with a transcription inhibitor (Actinomycin D) revealed that *dmrt2a* mRNA is stabilized in *celf1* morphants (Fig. 5B), meaning that Celf1 promotes *dmrt2a* mRNA decay in zebrafish embryos. These results therefore suggest that Celf1 is

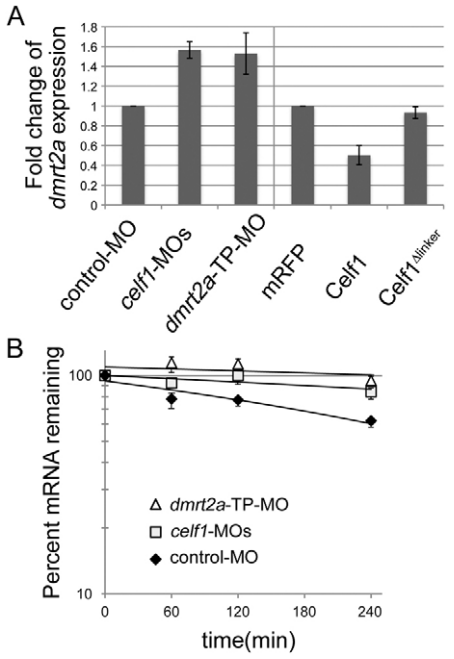

Fig. 5. Celf1 promotes *dmrt2a* mRNA decay in vivo. (**A**) Effect of Celf1 on *dmrt2a* expression in zebrafish embryos. Total RNAs extracted from embryos injected with control-MO, *celf1*-MOs, *dmrt2a*-TP-MO, *mRFP* mRNA, *celf1* mRNA or *celf1*$^{\Delta linker}$ mRNA at 12-14 hpf were subjected to qPCR for *dmrt2a* and *β-actin*. The samples were normalized to *β-actin* as a reference. (**B**) *dmrt2a* mRNA is stabilized in embryos injected with *celf1*-MOs or *dmrt2a*-TP-MO. Decay rate of *dmrt2a* mRNA was assessed in embryos injected with control-MO, *celf1*-MOs or *dmrt2a*-TP-MO by qPCR following transcription inhibition using Actinomycin D. The samples were normalized to *β-actin* as a reference. control-MO: $t_{1/2}$=317±11 minutes; *celf1*-MOs: $t_{1/2}$=835±3 minutes; *dmrt2a*-TP-MO: $t_{1/2}$=1487±4 minutes. Error bars represent s.d.

required to maintain *dmrt2a* mRNA at an appropriate level, and that Celf1 regulation of *dmrt2a* might contribute to proper symmetric somitogenesis and LR asymmetric patterning.

Celf1 regulation of *dmrt2a* is required to generate proper somite symmetry and LR asymmetric patterning

Target protector MOs (TP-MOs) have been developed to disrupt the interaction of specific microRNA-mRNA or protein-mRNA pairs (Choi et al., 2007; Cibois et al., 2010; Staton et al., 2011). To investigate the role of specific pairing between Celf1 and *dmrt2a* mRNA, we used *dmrt2a*-TP-MO, the sequence of which is complementary to the UGU repeats in the 3′UTR of *dmrt2a* mRNA. Injection of *dmrt2a*-TP-MO in zebrafish embryos interfered with the specific interaction between Celf1 and *dmrt2a* mRNA (Fig. 4C) and led to a 53% increase of *dmrt2a* mRNA (Fig. 5A), showing that *dmrt2a*-TP-MO protects *dmrt2a* mRNA from Celf1 in vivo. Notably, injection of *dmrt2a*-TP-MO only resulted in failures of somite symmetry and LR asymmetric patterning, whereas co-injection of *dmrt2a*-TP-MO and *dmrt2a* mRNA restored the failures caused by *dmrt2a*-TP-MO in a dose-dependent manner (Fig. 3C,D,G,H). These results indicate that Celf1-mediated regulation of *dmrt2a* is essential for somite symmetry and LR asymmetry during zebrafish development.

Based on these results, we hypothesized that *celf1* overexpression intensifies *dmrt2a* mRNA decay, eventually leading to LR asymmetric somitogenesis as well as a failure of LR patterning. If this is the case, either blocking the interaction between Celf1 and *dmrt2a* mRNA or increasing the amount of Dmrt2a should cancel the effects of *celf1* overexpression on somite symmetry and LR patterning. To test this, we co-injected *celf1* mRNA and either *dmrt2a*-TP-MO or the Celf1-resistant *dmrt2a* mRNA into zebrafish embryos and found substantial alleviation of the disruption of both symmetric somitogenesis (Fig. 6A-D,I) and cardiac laterality (Fig. 6E-H,J), relative to the effects of co-injection of *celf1* mRNA and either control-MO or *mRFP* mRNA. Hence, our results demonstrate that Celf1-mediated post-transcriptional regulation of *dmrt2a* is required to

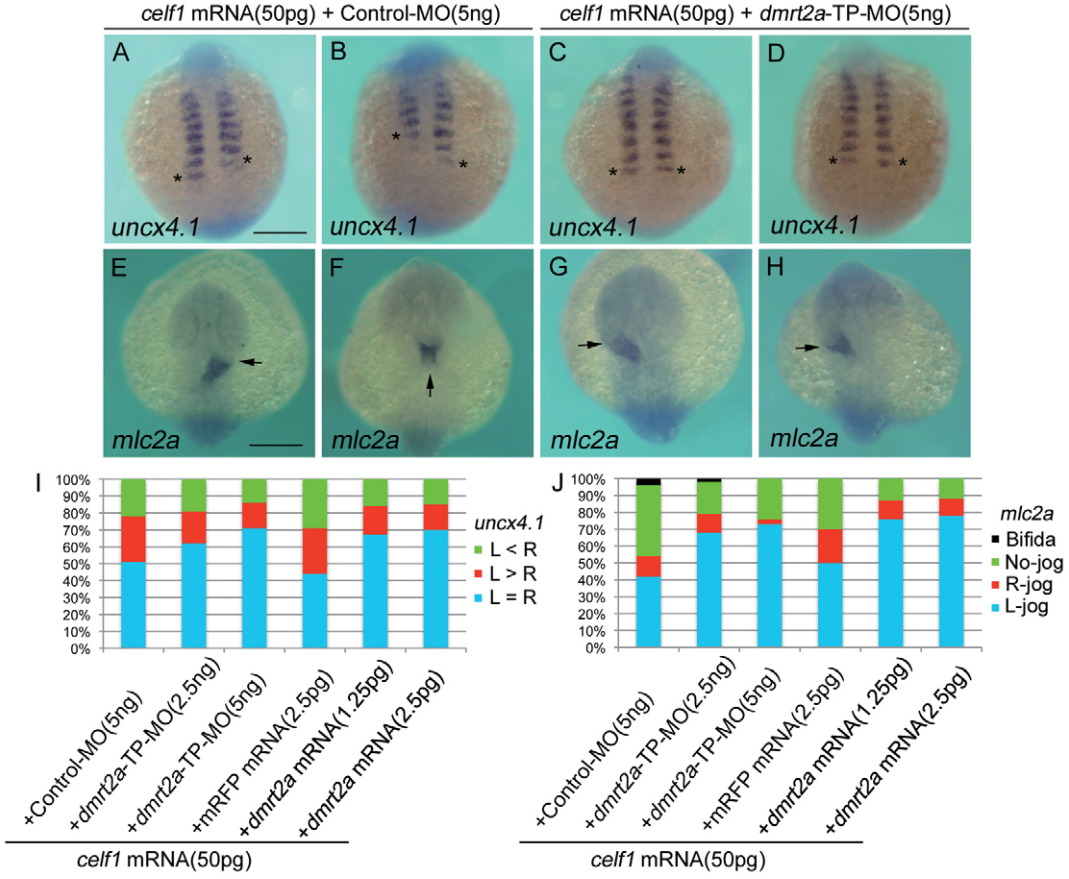

Fig. 6. Disruption of Celf1-*dmrt2a* mRNA interaction cancels the effects of *celf1* overexpression on somite symmetry and LR asymmetric patterning. (**A-D**) Representative images of *uncx4.1* expression showing left-biased (*celf1* mRNA plus control-MO; A), right-biased (*celf1* mRNA plus control-MO; B) or symmetric (*celf1* mRNA plus *dmrt2a*-TP-MO; C,D) somitogenesis in zebrafish embryos at 12-14 hpf. Dorsal view, anterior to the top. Asterisks mark the last-formed somite. (**E-H**) Representative images of *mlc2a* expression showing R-jog (*celf1* mRNA plus control-MO; E), no-jog (*celf1* mRNA plus control-MO; F) or L-jog (*celf1* mRNA plus *dmrt2a*-TP-MO; G,H) of the heart in embryos at 24-28 hpf. Dorsal view, anterior to the top. Arrows indicate the direction of heart jogging. (**I**) Percentages of symmetric (L=R), left-biased (L>R) or right-biased (L<R) asymmetric somitogenesis in embryos injected with 50 pg *celf1* mRNA and either 5 ng control-MO (*n*=70), 2.5 ng *dmrt2a-TP-MO* (*n*=43), 5 ng *dmrt2a*-TP-MO (*n*=79), 2.5 pg *mRFP* mRNA (*n*=55), 1.25 pg *dmrt2a* mRNA (*n*=69) or 2.5 pg *dmrt2a* mRNA (*n*=70) which lacks Celf1-binding site. (**J**) Percentages of L-jog, R-jog, no-jog, or cardia bifida of the heart in embryos injected with 50 pg *celf1* mRNA and either 5 ng control-MO (*n*=98), 2.5 ng *dmrt2a*-TP-MO (*n*=62), 5 ng *dmrt2a*-TP-MO (*n*=92), 2.5 pg *mRFP* mRNA (*n*=56), 1.25 pg *dmrt2a* mRNA (*n*=55) or 2.5 pg *dmrt2a* mRNA (*n*=62), which lacks Celf1-binding site. Scale bars: 200 μm.

control two key processes that generate a properly organized body during vertebrate development: symmetric somitogenesis and LR asymmetric patterning.

DISCUSSION

The vertebrate body displays invariant LR asymmetry, which is determined by symmetry-breaking events during early embryonic development. The other and contrasting feature of vertebrate body is the bilaterally symmetric arrangement of skeletal structures, including vertebrae and skeletal muscles, which arises from the metameric structures of the somites during early embryonic development. In this study, we characterize an RBP named Celf1 in zebrafish and show a previously unidentified role of Celf1 in coordinating symmetric somitogenesis and LR asymmetric patterning, which are essential processes for generating a properly organized body during embryonic development.

Phenotypes in embryos injected with 50 pg *celf1* mRNA point to crucial roles of Celf1 in the control of somite symmetry and LR patterning. However, it is noteworthy that Celf1 function is not exclusive for these processes. Injection of higher amounts of *celf1* mRNA (150 pg) led to additional defects including failures of epiboly and gastrulation at early stages and multiple defects, such as short body axis, abnormal segmentation, small head and small eyes at later stages (supplementary material Fig. S4). Such broad phenotypes suggest that Celf1 is involved in the regulation of multiple developmental processes in zebrafish. This is consistent with the fact that hundreds of Celf1's targets have been identified in various types of cells (Lee et al., 2010; Marquis et al., 2006; Mori et al., 2008; Rattenbacher et al., 2010; Suzuki et al., 2002; Takahashi et al., 2000). The observation that specific phenotypes could be segregated by lowering the amount of *celf1* mRNA might be a result of different thresholds of Celf1 activity.

In our model, Celf1 maintains *dmrt2a* mRNA at an appropriate level, and Celf1 regulation of *dmrt2a* is required to generate proper symmetric somitogenesis and LR asymmetric patterning. However, even in the presence of *dmrt2a*-TP-MO, 20-30% of *celf1*-overexpressing embryos display defects in symmetric somitogenesis and LR asymmetric patterning (Fig. 6I,J), suggesting that either efficacy or specificity of *dmrt2a*-TP-MO is low and/or that other targets of Celf1 contribute to regulation of these processes. Two lines of evidence argue against the first possibility: (1) the amount of *dmrt2a* mRNA in embryos injected with *dmrt2a*-TP-MO is similar to that of *celf1* morphants (Fig. 5A), showing high efficacy of *dmrt2a*-TP-MO; and (2) *dmrt2a*-TP-MO does not hamper the interaction of Celf1 with mRNA encoding either *myod* or *suppressor of hairless* (*rbpja* or *rbpjb*) (Fig. 4C), which are known targets of Celf1 in C2C12 cells (Lee et al., 2010) and in frog (Cibois et al., 2010; Gautier-Courteille et al., 2004), respectively, meaning that specificity of *dmrt2a*-TP-MO is also high. Importantly, frequencies of somite symmetric and LR patterning defects in embryos co-injected with 50 pg *celf1* mRNA and 5 ng *dmrt2a*-TP-MO (Fig. 6I,J) are similar to those of embryos injected with 5 ng *dmrt2a*-TP-MO alone (Fig. 3D,H). This similarity suggests that phenotypes seen in embryos co-injected with *celf1* mRNA and *dmrt2a*-TP-MO are caused by the dominant effect of *dmrt2a*-TP-MO, and thus supports the second possibility.

The zootype hypothesis proposed by Yost (Yost, 1999) suggests that major events in determining LR asymmetry, such as left-sided gene expression, are evolutionarily conserved, whereas the expression patterns, regulation and functions of genes are not necessarily conserved among vertebrates (Hirokawa et al., 2006; Yost, 1999). This notion is further supported by our findings that the functional interaction between Celf1 and *dmrt2a* mRNA might not be conserved among vertebrates because no putative Celf1-binding site is present within the 3′UTR of mouse and chick *Dmrt2*.

Conclusions

Hundreds of RBP-mRNA interactions have been predicted in vitro and in vivo, but just a few have been shown to have an in vivo function. Using an approach combining gain-of-function for RBP and protection of RBP-target interaction, we reveal the in vivo role of the specific RBP-mRNA pair in generating a properly organized body during zebrafish development. Our strategy therefore provides a powerful tool for understanding better the roles of specific RBP-mRNA pairs in vertebrate development and other experimental settings.

Acknowledgements

We are grateful to Thomas N. Sato, Yasukazu Nakahata, Naoyuki Inagaki and Kinichi Nakashima for advice, helpful discussions and critical reading of the manuscript. We also thank Ian Smith and Muh Chyi Chai for help in preparing the manuscript; Tomoko Murata, Maiko Yokouchi and Hiroko Shigesato for technical assistance; and Kunio Inoue for sharing anti-Celf1 antiserum.

Funding

This work was supported by Grants-in-Aid for Scientific Research [23111517 and 24681043 to T.M., 17017027 to Y.B. and T.M.] from the Ministry of Education, Culture, Sports, Science and Technology (MEXT), Japan and by the Global COE Program in Nara Institute of Science and Technology, MEXT, Japan.

Competing interests statement

The authors declare no competing financial interests.

Supplementary material

Supplementary material available online at
http://dev.biologists.org/lookup/suppl/doi:10.1242/dev.077263/-/DC1

References

Barreau, C., Paillard, L., Mereau, A. and Osborne, H. B. (2006). Mammalian CELF/Bruno-like RNA-binding proteins: molecular characteristics and biological functions. *Biochimie* **88**, 515-525.

Blake, W. J., Kaern, M., Cantor, C. R. and Collins, J. J. (2003). Noise in eukaryotic gene expression. *Nature* **422**, 633-637.

Choi, W. Y., Giraldez, A. J. and Schier, A. F. (2007). Target protectors reveal dampening and balancing of Nodal agonist and antagonist by miR-430. *Science* **318**, 271-274.

Cibois, M., Gautier-Courteille, C., Vallee, A. and Paillard, L. (2010). A strategy to analyze the phenotypic consequences of inhibiting the association of an RNA-binding protein with a specific RNA. *RNA* **16**, 10-15.

Cosson, B., Gautier-Courteille, C., Maniey, D., Ait-Ahmed, O., Lesomple, M., Osborne, H. B. and Paillard, L. (2006). Oligomerization of EDEN-BP is required for specific mRNA deadenylation and binding. *Biol. Cell* **98**, 653-665.

Elowitz, M. B., Levine, A. J., Siggia, E. D. and Swain, P. S. (2002). Stochastic gene expression in a single cell. *Science* **297**, 1183-1186.

Gautier-Courteille, C., Le Clainche, C., Barreau, C., Audic, Y., Graindorge, A., Maniey, D., Osborne, H. B. and Paillard, L. (2004). EDEN-BP-dependent post-transcriptional regulation of gene expression in Xenopus somitic segmentation. *Development* **131**, 6107-6117.

Gebauer, F. and Hentze, M. W. (2004). Molecular mechanisms of translational control. *Nat. Rev. Mol. Cell Biol.* **5**, 827-835.

Hashimoto, Y., Suzuki, H., Kageyama, Y., Yasuda, K. and Inoue, K. (2006). Bruno-like protein is localized to zebrafish germ plasm during the early cleavage stages. *Gene Expr. Patterns* **6**, 201-205.

Hirokawa, N., Tanaka, Y., Okada, Y. and Takeda, S. (2006). Nodal flow and the generation of left-right asymmetry. *Cell* **125**, 33-45.

Kawakami, Y., Raya, A., Raya, R. M., Rodriguez-Esteban, C. and Belmonte, J. C. (2005). Retinoic acid signalling links left-right asymmetric patterning and bilaterally symmetric somitogenesis in the zebrafish embryo. *Nature* **435**, 165-171.

Kress, C., Gautier-Courteille, C., Osborne, H. B., Babinet, C. and Paillard, L. (2007). Inactivation of CUG-BP1/CELF1 causes growth, viability, and spermatogenesis defects in mice. *Mol. Cell. Biol.* **27**, 1146-1157.

Lee, J. E., Lee, J. Y., Wilusz, J., Tian, B. and Wilusz, C. J. (2010). Systematic analysis of cis-elements in unstable mRNAs demonstrates that CUGBP1 is a key regulator of mRNA decay in muscle cells. *PLoS ONE* **5**, e11201.
Marquis, J., Paillard, L., Audic, Y., Cosson, B., Danos, O., Le Bec, C. and Osborne, H. B. (2006). CUG-BP1/CELF1 requires UGU-rich sequences for high-affinity binding. *Biochem. J.* **400**, 291-301.
Matsui, T., Raya, A., Kawakami, Y., Callol-Massot, C., Capdevila, J., Rodriguez-Esteban, C. and Izpisua Belmonte, J. C. (2005). Noncanonical Wnt signaling regulates midline convergence of organ primordia during zebrafish development. *Genes Dev.* **19**, 164-175.
Matsui, T., Thitamadee, S., Murata, T., Kakinuma, H., Nabetani, T., Hirabayashi, Y., Hirate, Y., Okamoto, H. and Bessho, Y. (2011). Canopy1, a positive feedback regulator of FGF signaling, controls progenitor cell clustering during Kupffer's vesicle organogenesis. *Proc. Natl. Acad. Sci. USA* **108**, 9881-9886.
Meng, A., Moore, B., Tang, H., Yuan, B. and Lin, S. (1999). A Drosophila doublesex-related gene, terra, is involved in somitogenesis in vertebrates. *Development* **126**, 1259-1268.
Mori, D., Sasagawa, N., Kino, Y. and Ishiura, S. (2008). Quantitative analysis of CUG-BP1 binding to RNA repeats. *J. Biochem.* **143**, 377-383.
Naiche, L. A., Harrelson, Z., Kelly, R. G. and Papaioannou, V. E. (2005). T-box genes in vertebrate development. *Annu. Rev. Genet.* **39**, 219-239.
Oishi, I., Kawakami, Y., Raya, A., Callol-Massot, C. and Izpisua Belmonte, J. C. (2006). Regulation of primary cilia formation and left-right patterning in zebrafish by a noncanonical Wnt signaling mediator, duboraya. *Nat. Genet.* **38**, 1316-1322.
Rattenbacher, B., Beisang, D., Wiesner, D. L., Jeschke, J. C., von Hohenberg, M., St Louis-Vlasova, I. A. and Bohjanen, P. R. (2010). Analysis of CUGBP1 targets identifies GU-repeat sequences that mediate rapid mRNA decay. *Mol. Cell. Biol.* **30**, 3970-3980.
Saude, L., Lourenco, R., Goncalves, A. and Palmeirim, I. (2005). terra is a left-right asymmetry gene required for left-right synchronization of the segmentation clock. *Nat. Cell. Biol.* **7**, 918-920.
Schier, A. F. and Talbot, W. S. (2005). Molecular genetics of axis formation in zebrafish. *Annu. Rev. Genet.* **39**, 561-613.
Shivdasani, R. A. (2002). Molecular regulation of vertebrate early endoderm development. *Dev. Biol.* **249**, 191-203.
Staton, A. A., Knaut, H. and Giraldez, A. J. (2011). miRNA regulation of Sdf1 chemokine signaling provides genetic robustness to germ cell migration. *Nat. Genet.* **43**, 204-211.
Suzuki, H., Jin, Y., Otani, H., Yasuda, K. and Inoue, K. (2002). Regulation of alternative splicing of α-actinin transcript by Brumo-like proteins. *Genes Cells* **7**, 133-141.
Takahashi, N., Sasagawa, N., Suzuki, K. and Ishiura, S. (2000). The CUG-binding protein binds specifically to UG dinucleotide repeats in a yeast three-hybrid system. *Biochem. Biophys. Res. Commun.* **277**, 518-523.
Vermot, J. and Pourquie, O. (2005). Retinoic acid coordinates somitogenesis and left-right patterning in vertebrate embryos. *Nature* **435**, 215-220.
Vermot, J., Gallego Llamas, J., Fraulob, V., Niederreither, K., Chambon, P. and Dolle, P. (2005). Retinoic acid controls the bilateral symmetry of somite formation in the mouse embryo. *Science* **308**, 563-566.
Vilhais-Neto, G. C., Maruhashi, M., Smith, K. T., Vasseur-Cognet, M., Peterson, A. S., Workman, J. L. and Pourquie, O. (2010). Rere controls retinoic acid signalling and somite bilateral symmetry. *Nature* **463**, 953-957.
Vlasova, I. A., Tahoe, N. M., Fan, D., Larsson, O., Rattenbacher, B., Sternjohn, J. R., Vasdewani, J., Karypis, G., Reilly, C. S., Bitterman, P. B. et al. (2008). Conserved GU-rich elements mediate mRNA decay by binding to CUG-binding protein 1. *Mol. Cell* **29**, 263-270.
Yost, H. J. (1999). Diverse initiation in a conserved left-right pathway? *Curr. Opin. Genet. Dev.* **9**, 422-426.

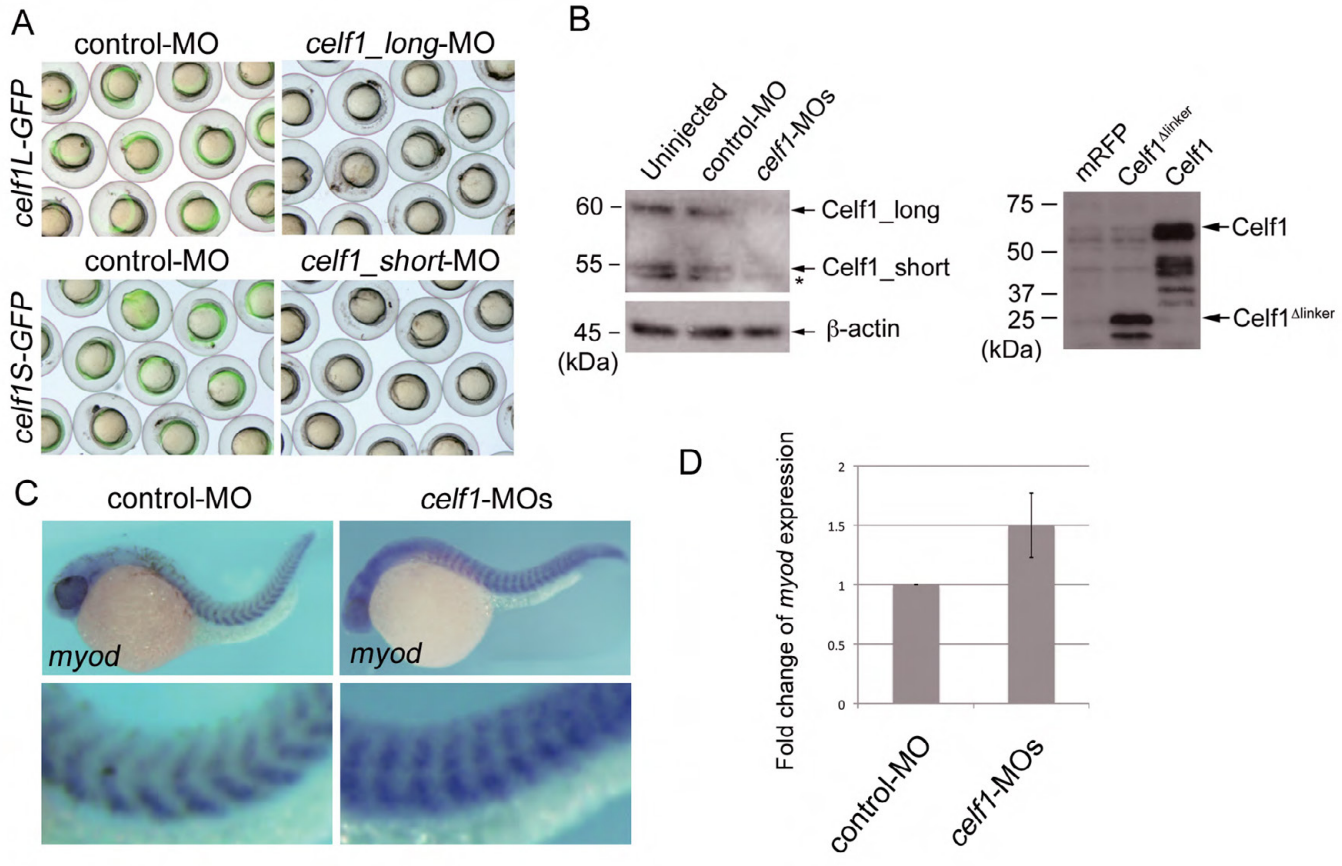

Fig. S1. *celf1* plays a crucial role in symmetric somitogenesis and LR asymmetric patterning. (**A**) *celf1_long*-MO and *celf1_short*-MO inhibited the expression of *celf1L*-GFP and *celf1S*-GFP, respectively. (**B**) Western blotting using anti-Celf1 antiserum. Left panel: co-injection of *celf1_long*-MO with *celf1_short*-MO (*celf1*-MOs) inhibited the expression of both forms of endogenous Celf1 in zebrafish embryos. The asterisk indicates a non-specific band. Right panel: Celf1 and Celf1$^{\Delta linker}$ proteins were detected in Celf1- and Celf1$^{\Delta linker}$-overexpressing embryos, respectively. (**C**) Representative images of *myod* expression demonstrating normal (left; control-MO, *n*=105) or abnormal (right; *celf1*-MOs, *n*=88) somitogenesis in embryos at 24-28 hpf. Higher magnification images (lower panels) highlight somites. Knockdown of *celf1* resulted in a mild loss of the chevron shape of somites (94%). (**D**) Upregulation of *myod* expression in *celf1* morphants. qPCR assay revealed that *celf1* knockdown resulted in a 50% increase of *myod* expression in zebrafish embryos, suggesting that *myod* is a target of Celf1 not only in C2C12 (Lee et al., 2010) but also in zebrafish.

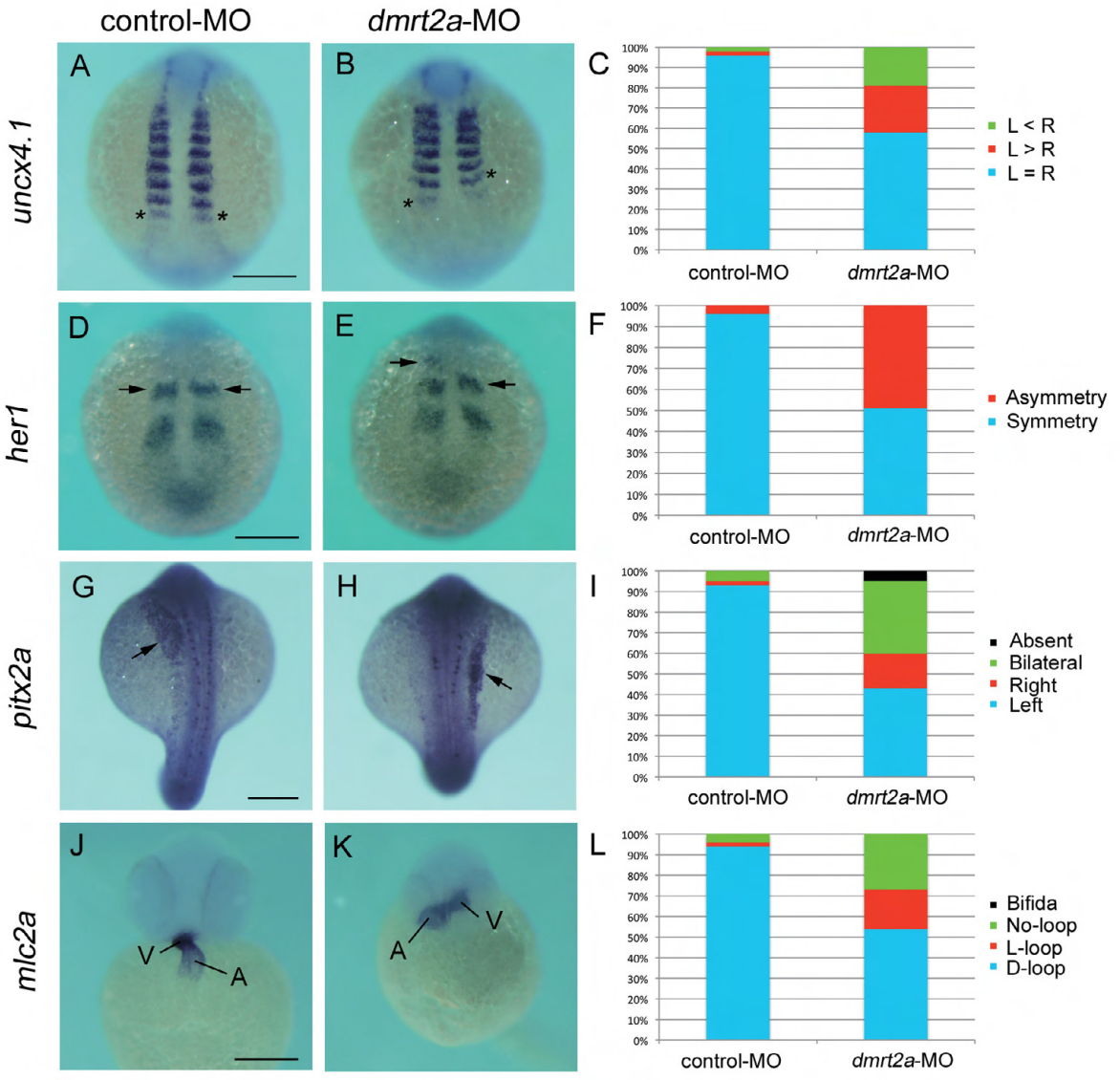

Fig. S2. Knockdown of *dmrt2a* yields defects similar to those seen in celf1-overexpressing embryos. (**A**,**B**,**D**,**E**,**G**,**H**,**J**,**K**) In situ hybridization for *uncx4.1* (A,B), *her1* (D,E), *pitx2a* (G,H) or *mlc2a* (J,K) in control-MO-injected (A,D,G,J) or *dmrt2a*-MO-injected (B,E,H,K) embryos. Asterisks in A and B mark the last-formed somite. Arrows in D, F, G and H indicate the position of the anterior strip of *her1* and *pitx2a* expression in the lateral plate mesoderm, respectively. A, atrium; V, ventricle. Scale bar: 200 µm. (**C**) Percentages of symmetric (L=R), left-biased (L>R) or right-biased (L<R) asymmetric somitogenesis in embryos injected with control-MO (*n*=44) or *dmrt2a*-MO (*n*=53). (**F**) Percentages of symmetric and asymmetric *her1* oscillation in embryos injected with control-MO (n=48) or *dmrt2a*-MO (*n*=51). (**I**) Percentages of left-sided, right-sided, bilateral, or no (absent) expression of *pitx2a* in embryos injected with control-MO (*n*=59) or *dmrt2a*-MO (*n*=46). (**L**) Percentages of D-loop, L-loop, no-loop or cardia bifida of the heart in embryos injected with control-MO (*n*=58) or *dmrt2a*-MO (*n*=78).

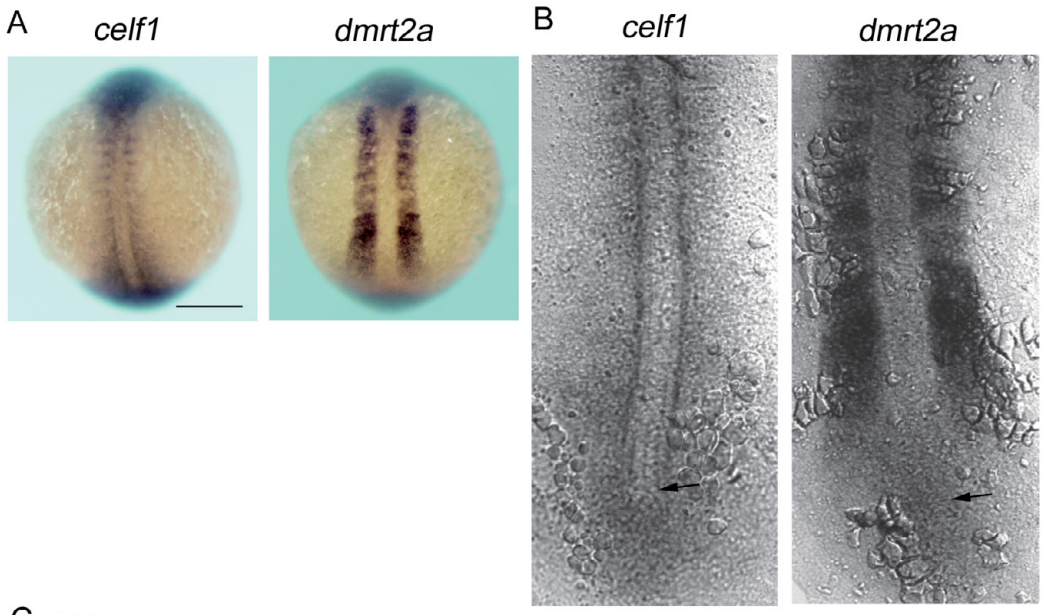

C 3'UTR of *dmrt2a*

ggcuucuugc uaacaacaac agcaaaccuu aaaaguaaaa uuguaacuuu
gugcugauug uauauuuauu uucaaaugca uauuuuuuaa guuuauauaa
auacaagaca gaaaaagaug auccuaggaa uaaucaaaag ggcauaugug
cagcuuuaug gacacuucug uguguauaua uauauauaaa uaaauguaca
uaacauuuca gacaugcaug uuguacauua aaauauauga uaaugugag
aguauuuaau uguaaaugu aauuuugcua cauuaaaaau gucaauaaaa
ugaaauuucg aaauaaaaaa aaaaaaaaaa aaaaaaaaaa aaaaaaaaaa
aaaaaaaaaa aa

D

zebrafish *myod*	uaguuuguugugucuuguguuaaacuuuauauuua
mouse *MyoD*	uuuuuguuguuguuguuguaguccuucaguuguuu
human *MyoD*	uuuuuguaauacuuuuguaaucuauuccuguaaau

E

zebrafish *rbpja*	auguuuucaguguuauuuuucucuucuucaauugu
zebrafish *rbpjb*	uaauaguguuuugugauuuucuuuuuuauguacag
Xenopus Rbpj	uguucuuuuuuuuuuuuguuuuguuuguguuguu

Fig. S3. *dmrt2a* mRNA is a target of Celf1. (**A**,**B**) *celf1* (left) or *dmrt2a* (right) expression in zebrafish embryos at 12-14 hpf. (A) Dorsal view of whole-mount embryos. Scale bar: 200 μm. (B) Dorsal view of flat-mounted embryos. Arrows mark the position of Kupffer's vesicle. (**C**) Sequence of the 3′UTR of *dmrt2a* mRNA. Red letters are the putative Celf1-binding site including UGU repeats (underlined), and U- and A-rich sequences. The 35 nucleotides were used as a probe named *dmrt2a*_wildtype for an in vitro binding assay (see also Fig. 4A). (**D**,**E**) The putative Celf1-binding sites including UGU repeats (underlined) and U- and A-rich sequences were found within 3′UTR of *myod* (D) or *rbpj* (E) mRNA, but sequence homology was low among species.

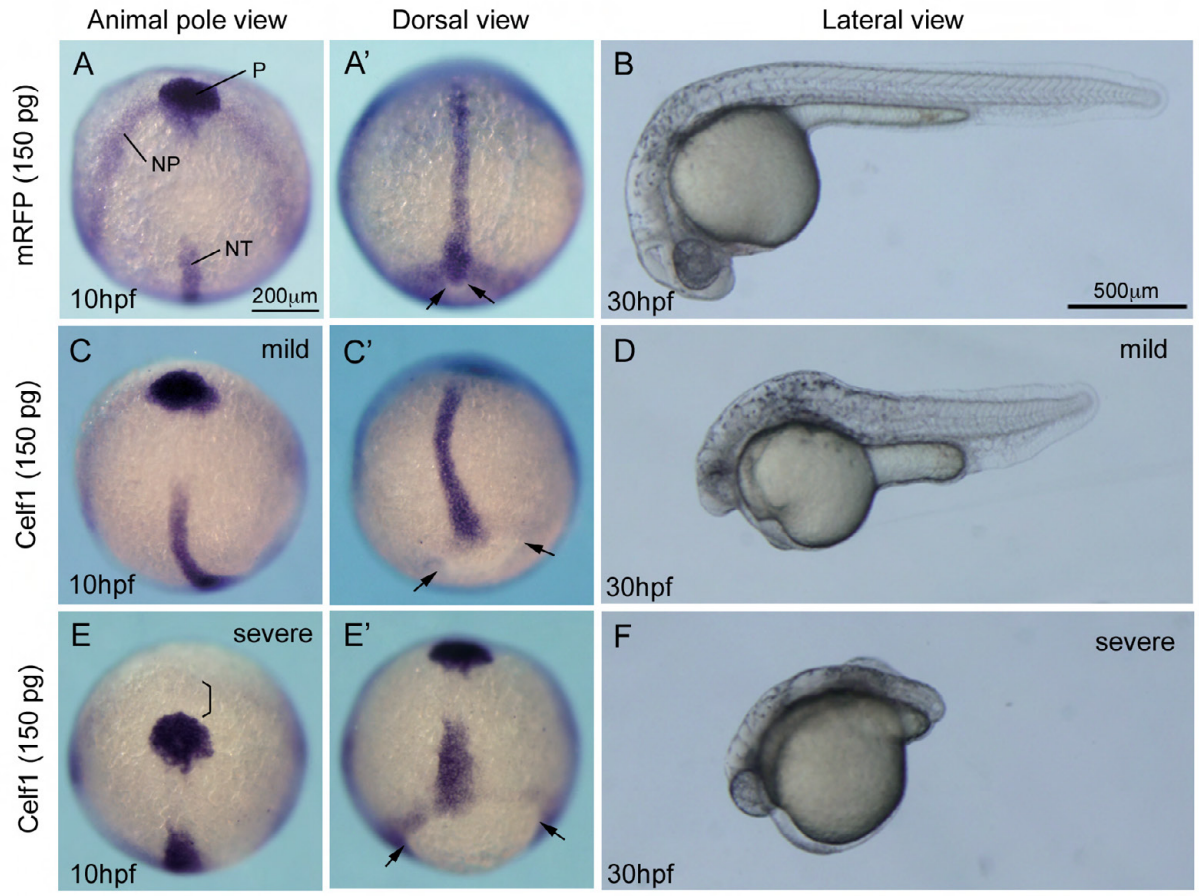

Fig. S4. Higher amounts of *celf1* mRNA lead to additional defects in zebrafish. (**A**,**C**,**E**) Expression of *hgg1* (P, polster), *dlx3* (NP, anterior edge of the neural plate) or *ntl* (NT, notochord) in embryos injected with *mRFP* (A) or *celf1* (C,E) mRNAs (150 pg). Animal pole view. Scale bar: 200 μm. (**A′**,**C′**,**E′**) Dorsal view of the embryo, anterior to the top. Injection of 150 pg *celf1* mRNA resulted in the formation of bended (C′) or short (E′) notochord. The polster did not reach the anterior edge of the neural plate (bracket in E). Epiboly was incomplete (C′,E′). Arrows in A′, C′ and E′ mark edge of the yolk plug. (**B**,**D**,**F**) Lateral view of embryos injected with *mRFP* (B) or *celf1* (D, F) mRNAs (150 pg) at 30 hpf. Various phenotypes, such as short tails, segmentation defects, small eyes, small heads and less pigmentation, were observed (D,F).